The effect of morphology on the temperature-dependent photoluminescence quantum efficiency of the conjugated polymer poly(9, 9-dioctylfluorene)

2002 J. Phys.: Condens. Matter 14 9975

(http://iopscience.iop.org/0953-8984/14/42/310)

INSTITUTE OF PHYSICS PUBLISHING JOURNAL OF PHYSICS: CONDENSED MATTER

J. Phys.: Condens. Matter **14** (2002) 9975–9986 PII: S0953-8984(02)37046-2

The effect of morphology on the temperature-dependent photoluminescence quantum efficiency of the conjugated polymer poly(9, 9-dioctylfluorene)

M Ariu[1], D G Lidzey[1,4], M Sims[1], A J Cadby[1], P A Lane[2] and D D C Bradley[3]

[1] The University of Sheffield, Department of Physics and Astronomy, Hicks Building, Hounsfield Road, Sheffield S3 7RH, UK
[2] C S Draper Laboratory, 555 Technology Square, Cambridge, MA 02139, USA
[3] Imperial College of Science, Technology and Medicine, Blackett Laboratory, Prince Consort Road, London SW7 2BZ, UK

E-mail: d.g.lidzey@sheffield.ac.uk

Received 15 May 2002
Published 11 October 2002
Online at stacks.iop.org/JPhysCM/14/9975

Abstract

We have measured the temperature-dependent photoluminescence quantum yields (PLQYs) of poly(9, 9-dioctylfluorene) (PFO) films with four morphologies, namely as-spin-coated (SC) glass, quenched nematic glass, crystalline, and vapour-treated SC glass containing a fraction of 2_1 helix conformation (β-phase) chains. We find that the room temperature PLQYs of the as-SC, crystalline, and quenched films all increase as the temperature is reduced. However, the PLQY of the film containing β-phase chains decreases at temperatures below 150 K. Via temperature-dependent photoinduced absorption measurements, we show that the polaron population in films containing β-phase PFO chains grows as the temperature is reduced, and is significantly larger than in films with any of the other morphologies. Because of the smaller HOMO–LUMO (highest occupied molecular orbital–lowest unoccupied molecular orbital) energy gap of the β-phase chains compared to chains in the surrounding glassy PFO matrix, they act as recombination sites for excitons, and as traps for polarons. Hence at low temperatures, the polarons become strongly localized on these chains, where they quench the singlet excitons and reduce the PLQY.

Conjugated polymers are a class of materials that has been widely studied as regards applications in light-emitting diodes and displays [1–9]. The electroluminescence efficiency

[4] Author to whom any correspondence should be addressed.

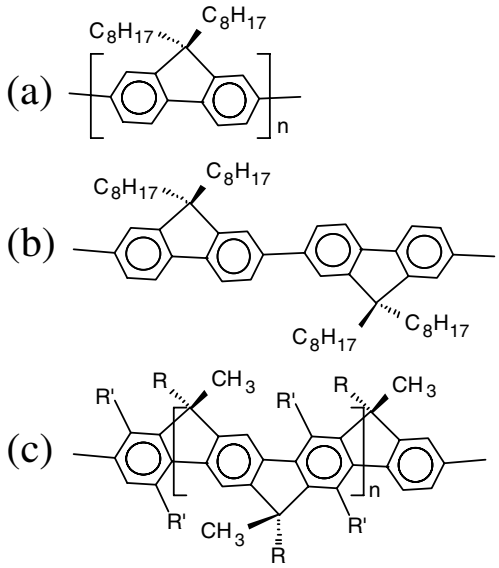

Figure 1. (a) The chemical structure of poly(9, 9-dioctylfluorene), (b) the 2_1 helical conformation or β-phase chain structure, (c) the chemical structure of a related ladder poly(p-phenylene), namely Me-LPPP where R = 1, 4-C_6H_4-*n*-$C_{10}H_{12}$ and R′ = *n*-C_6H_{13}.

of such devices is fundamentally limited by the radiative recombination efficiency of singlet excitons. It is thus of significant importance to understand the nature of the non-radiative channels that compete with radiative emission. By gaining a full understanding of the nature of emission quenching processes, it may be possible to design and synthesize new materials having higher fluorescence efficiencies, and perhaps create optoelectronic devices with increased electroluminescence efficiency.

Our previous work using a scanning tunnelling microscope to inject charges into a conjugated polymer demonstrated that the efficiency of exciton generation and thus electroluminescence emission intensity varied strongly over length scales of a few nanometres [10]. This observation suggested that the local molecular order and conformation played a key role in determining the processes surrounding both charge transport and exciton radiative recombination. Such conclusions are in accord with other reports in the literature [11–13]. To gain further insight into the effect of molecular conformation on the photoluminescence quantum yield (PLQY), we have studied the emission efficiency of the polymer poly(9, 9-dioctylfluorene) (PFO) (see the chemical structure in figure 1(a)). This material is particularly interesting for the study of photophysical processes, as it can be prepared in a number of distinct morphologies using either thermal or vapour exposure protocols. A comparison of the PLQYs of PFO films that differ only as regards their morphology allows us to eliminate the influence of chemical composition (which would be important when comparing the PLQYs of *different* polymers). We can thus more readily identify the effects of morphology on non-radiative channels. As we demonstrate below, strong nanoscale inhomogeneity in the energy gap of polymer chains can result in the stabilization of electron and hole polarons, which quench the PLQY of PFO at low temperatures.

PFO films were prepared for PLQY measurements with four different morphologies: namely as-spin-coated (SC) glass, quenched nematic glass, crystalline, and vapour-treated SC glass containing a fraction of 2_1 helix conformation (β-phase) chains (see [14] and [15] for a detailed discussion on the different structural forms of PFO). SC glass films were prepared

by dissolving PFO at 20 mg ml^{-1} in chloroform and then spin-coating to create a glassy film 350 nm in thickness. Chloroform was used as a solvent instead of toluene or xylene (as in our previous work [15, 16]). It was found that chloroform completely suppresses the β-phase formation whilst when other solvents were used a small concentration of β-phase was formed even in the fresh SC films. For photoinduced absorption (PA) measurements it was necessary to use much thicker films to detect a significant change in absorption. This was achieved by drop-casting a PFO solution from chloroform to create a film having a thickness of 5 ± 0.5 μm. Quenched nematic glass films were prepared by heating as-SC films into their nematic mesophase and then rapidly cooling to 77 K. Crystalline films were prepared by heating as-SC films to 220 °C and then slowly cooling them (at 0.1 °C min^{-1}) to room temperature. β-phase chain conformations were induced in as-SC glassy films by exposing them to toluene vapour. This exposure causes a swelling stress to be applied to the film, which induces an elongation in a fraction of the polymer chains, causing them to adopt a 2_1 helix conformation. The structure of fibres drawn from the nematic melt, quenched, and then subjected to vapour exposure was studied by x-ray diffraction [14, 17] and it was found that β-phase chains are highly extended with a conjugation length of approximately 30 monomer units. The 2_1 helix conformation has a pitch that corresponds to two monomer units; i.e. the angle between the plane of two adjacent fluorene units is 180° (see figure 1(b)). The structure is thus similar to that of the ladder polymer Me-LPPP, whose structure is shown in figure 1(c). Note that in Me-LPPP, the planarity of the polymer is locked in as a result of the chemical structure of polymer backbone.

The quenched nematic glass, crystalline, and β-phase morphologies have been induced in the drop-cast films using the same procedure as described above for the as-SC glass film. We believe that the drop-casting process does not introduce any significant structural difference in the film compared to the as-SC glass: wide-angle x-ray diffraction measurements on drop-cast films do not show any crystallization peak caused by slow solvent evaporation. Furthermore, the slow solvent evaporation that occurs during the drop-casting is analogous to the vapour exposure treatment performed to induce the β-phase. We therefore conclude that the β-phase SC glass and the β-phase drop-cast films are very similar. In the case of the drop-cast nematic glass and crystalline morphologies, the films are driven into the nematic liquid phase and thus they lose any possible memory of structures induced by the drop-casting process.

We have measured the PLQY and PA spectra of PFO films in the four different morphologies, as a function of temperature between 298 and 10 K. A schematic diagram of the PA apparatus used is shown in figure 2(a). The films were optically pumped using the 351 nm line of an argon-ion laser (130 W m^{-2}) chopped mechanically at 300 Hz. Standard phase-sensitive detection was used to measure the change in transmission of the light from a tungsten lamp through the sample. Note that this experiment detects states whose order-of-magnitude lifetime accords with the inverse modulation frequency, namely those with lifetimes in the range $10\ \mu s \leqslant \tau \lesssim 100$ ms. The PLQY of PFO was measured at room temperature using a nitrogen-gas-filled integrating sphere as previously described [18]. Films were excited at 354 nm using a HeCd laser having a power density of 100 W m^{-2} (very similar to that used in the PA measurements). Fluorescence was collected using a fibre-bundle link from the integrating sphere to a scanning monochromator with a photomultiplier (PMT) detector. The optical response (in terms of volts per photon) of the integrating sphere and monochromator with PMT detector system had been previously calibrated with reference to a standard lamp calibrated by the National Physical Laboratory. We estimate the systematic error in our PLQY determination to be $\pm 10\%$.

To measure the PLQY at low temperature, the PFO films were placed in a cryostat and photoluminescence was excited using a HeCd laser (see the schematic diagram in figure 2(b)).

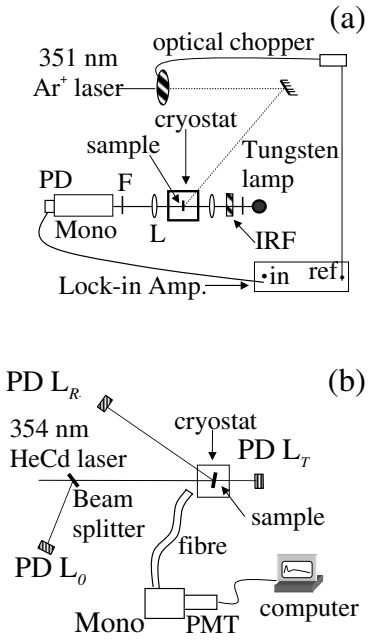

Figure 2. Schematic diagrams of the apparatus used to measure (a) PA spectra and (b) PLQYs at low temperature. Key: L = lens, F = UV filter, IRF = infrared rejection filter, PD = photodiode, Mono = monochromator, in and ref. = input and reference channels of the lock-in amplifier, PMT = photomultiplier.

The photoluminescence was collected at one angle (≈45°) from the surface normal using a fibre bundle, and then delivered to the monochromator with the PMT detector. Three photodiodes were used to monitor the incident laser power (L_0), and the power of the excitation light either reflected from (L_R) or transmitted through (L_T) the PFO film. This allowed the power of the laser light absorbed by the PFO to be directly calculated. The relative number of photons emitted by the PFO as a function of wavelength ($I(\lambda)$) can then be related to the PLQY using

$$QY = \frac{N_e}{N_a} = C\frac{\int I(\lambda)\,\mathrm{d}\lambda}{L_0 - L_T - L_R} \tag{1}$$

where N_e is the number of emitted photons, N_a is the number of absorbed photons, and C is a *geometrical constant* which accounts for the fact that only a small fraction of the photoluminescence from the PFO was collected by the fibre bundle. The constant C was determined by firstly measuring the PLQY of a PFO thin film at room temperature using the integrating sphere, and then transferring the PFO film to the cryostat which was also held at room temperature, and then measuring $\int I(\lambda)\,\mathrm{d}\lambda$, L_0, L_R, and L_T. Measurements of the PLQY were then made as the temperature was reduced from 300 to 10 K.

Our method assumes that the geometric constant C remains unchanged as a function of temperature. It has been argued, however, that in certain circumstances this is not a good approximation [19–21]. In particular, if the species that emits at room temperature is different from that which emits at low temperature, the spatial distribution of photoluminescence is likely to change as a result of the dipole moments of the two emitting species having different orientations. We consider that this is not the case in our thin films of PFO. As we show below, the photoluminescence emission does not indicate the existence of a new emissive species for any of the different film morphologies at low temperature. In addition, ellipsometry measurements

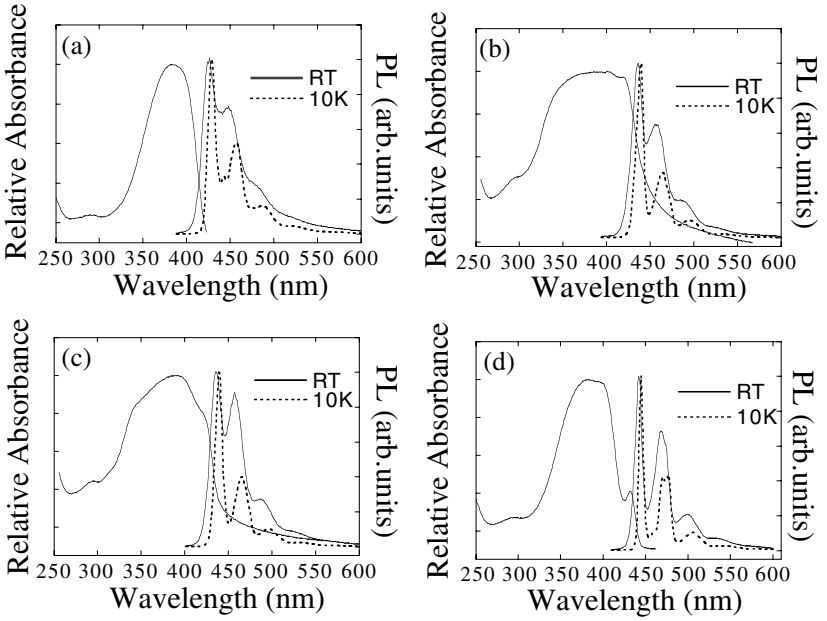

Figure 3. The absorption and PL spectra measured at room temperature and at 10 K for PFO films with four different morphologies, namely (a) as-SC glass, (b) quenched nematic glass, (c) crystalline, and (d) vapour-treated SC glass containing a fraction of β-phase chains.

have shown that SC PFO films are highly homogeneous [22]. Crystalline PFO films are likely to be less homogeneous but AFM measurements indicate that the crystallites are randomly oriented (we are not dealing here with aligned films). We thus expect, even for crystalline films, the total anisotropy to be very small. Note also that the PL was collected from an area of the sample (3 mm^2) that was very much bigger than the typical crystallite dimensions (100 nm). We thus believe that the difficulties discussed in [19] and [21], that relate to PLQY measurements on ultrathin, highly ordered films of crystalline oligomeric materials, do not apply in this case.

Figures 3(a)–(d) show the absorption and photoluminescence spectra, measured both at room temperature and at 10 K, of PFO films prepared in each of the four morphologies. It can be seen that the as-SC glass film has a relatively narrow absorption band peaking at 380 nm, with a full width at half-maximum (FWHM) of 70 nm. The absorption spectrum of the PFO film that contains the β-phase chains shows an additional well-resolved absorption peak at 436 nm, which has been assigned to the 0–0 absorption band of the 2_1 helix conformation [23]. This peak occurs at a slightly lower energy than the HOMO–LUMO transition peak of the non-helical PFO chains forming the bulk of the film. The fraction of chains in the helical conformation can be estimated from the relative contribution of the red-shifted absorption peak. For this sample we estimate a fraction of 13%. A PFO film containing the highly conjugated β-phase chains can thus be viewed as a 'self-doped' system where a fraction of chains with a lower energy gap are intimately dispersed in a 'matrix' of polymer chains with a larger energy gap. We find that almost all of the excitons generated in the 'matrix' transfer to the lower-energy-gap β-phase chains, even if the film contains only a 1 or 2% fraction of these chains. This energy migration is evident if one compares the PL emission spectrum of the film containing the β-phase chains (figure 3(d)) with that of a typical as-SC film (figure 3(a)). It can

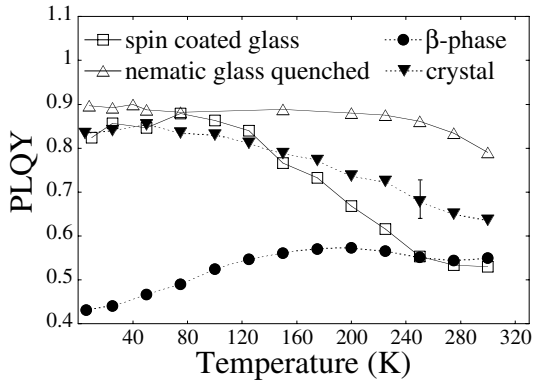

Figure 4. The temperature dependences of the PLQYs for PFO films with four different morphologies.

be seen that the two PL spectra are quite different: the β-phase film shows a red-shift of $\approx$17 nm in its peak emission wavelength compared to that of the as-SC film. The emission spectrum of the β-phase-containing film is also characterized by relatively narrow emission peaks: the FWHM of the 0–0 transition of the β-phase-containing film is 5 nm at 10 K compared to 13 nm for the as-SC film at the same temperature. The relative narrowness of the 0–0 emission peak mirrors the situation found for Me-LPPP, consistent with a molecular conformation that has a high degree of structural rigidity.

The absorption spectra of PFO films, for both the nematic glass and crystalline morphologies, display a small red-shift in absorption compared to the as-SC film, and both have a significantly broader linewidth (FWHM = 120 nm). Broadening and red-shift of the absorption can be explained by changes in conjugation length of a fraction of polymer chains in the film and also by increases in the dielectric constant due to the higher film density of the nematic glass and the crystalline phase with respect to the as-SC glass film. At present we cannot conclusively discriminate between these two effects. It is clear that a deeper understanding of the electronic properties of such films will only be gained via detailed molecular modelling which is able to account for intermolecular interactions. In both of these morphologies, it can be seen that the absorption tail extends to significantly longer wavelengths. We believe that this feature results from increased scattering in the films rather than from direct absorption. The assignment of scattering within the films is further confirmed by their slightly frosted appearance.

Figure 4 shows the PLQY for each of the four different film morphologies as a function of temperature. The room temperature PLQYs for the different films are as follows: $\Phi = 53\%$ for the as-SC film, 55% for the β-phase-containing film, 63% for the crystalline film, and 78% for the nematic glass film. Previous measurements of PLQY for as-SC films of PFO are in broad agreement with the value measured here [16, 24]. The PL decay lifetimes measured at the 0–0 peak for the four morphologies are as follows: 430 ± 10 ps for both the as-SC glass and the β-phase-containing film, 540 ± 10 ps for the crystal, and 490 ± 10 ps for the nematic glass. The increase in the quantum efficiency for the glass and the crystal is thus accompanied by an increase in the observed fluorescence decay time. This indicates that differences in room temperature PLQY between the different morphologies can be understood on the basis of changes in the non-radiative decay channels rather than significant differences in the radiative rate. At present we cannot quantitatively explain why the crystalline and glassy phases have

relatively enhanced quantum efficiencies with respect to the other two phases. However, it is interesting to note that the nematic glass film has a higher PLQY than the crystalline film. It may be that grain boundaries in the crystalline film act as non-radiative quenching sites, as has been observed in other molecular systems [11–13].

As the temperature is reduced from room temperature to 10 K, the PLQYs of the nematic glass and crystalline films rise by 13 and 28% respectively, while the PLQY for the as-SC film rises by 55%. In contrast, the PLQY of the film containing β-phase chains reduces by 20%. Increases in the PLQY in polymeric films can be explained by hindered exciton migration at low temperature and/or freezing out of a thermally activated process. It has been shown that energy transport in disordered organic semiconductors occurs by a two-step process, involving both dipole–dipole coupling (Förster transfer) and thermally assisted migration [25, 26]. Hence at low temperature the volume of space that an exciton can sample is reduced, which reduces the probability for interaction with non-radiative traps or defects. Such defects can be oxidized (or otherwise degraded) segments of a polymer chain, chain ends, or trapped charges [27]. The reduced interaction volume at low temperature is reflected in an increase of the PLQY.

It is interesting to note that at temperatures approaching 10 K, the PLQYs of the nematic glass, crystalline, and as-SC films appear to approach very similar limiting values, $\Phi = 85 \pm 10\%$. It therefore appears that at low temperatures, the thermally assisted exciton migration in films with each of these morphologies is reduced to the point that the excitons are sufficiently localized to be unlikely to reach a quenching site within their radiative lifetime. In this limiting case, the 'intrinsic' PLQYs of each of the film morphologies are approximately the same.

It is clear that a different process is important in PFO films containing β-phase polymer chains. As the chemical compositions and polymer characteristics (degree of polymerization, polydispersity, etc) of the samples used to prepare each of the PFO films are identical, the additional non-radiative processes observed in the β-phase appear to originate from the effects of the polymer film nanostructure. We summarize the possible non-radiative exciton decay channels as follows:

(a) Decay at structural and chemical defects.
(b) Singlet–singlet annihilation.
(c) Intersystem crossing:

$$S_1 \rightarrow T_n + \text{phonons} \rightarrow T_1 + \text{phonons} \rightarrow S_0 + \text{phonons}.$$

(d) Singlet–triplet quenching:

$$S_1 + T_n \rightarrow S_0 + T_1 + \text{phonons} \rightarrow S_0 + \text{phonons}.$$

(e) Singlet–polaron quenching:

$$S_1 + P^{\pm} \rightarrow S_0 + P^{\pm} + \text{phonons}.$$

Here S_1 refers to the first excited singlet exciton state, S_0 to the ground singlet state, T_n to a triplet exciton in the nth excited state, and $P^{\pm}$ to a hole (+)/electron (−) polaron [28]. We can exclude the possibility of channel (a) being responsible for the *additional* non-radiative channels in the β-phase-containing film, since the PFO used to fabricate this sample was chemically identical to that used to make the films with the other morphologies. In addition, we do not anticipate channel (b) to be important, as the volume excitation rate at which the PLQY measurements were performed was $\approx 10^{21}$ photons cm^{-3} s^{-1}. At this low excitation density the PL grows linearly with the excitation power, consistent with monomolecular recombination. We rule out channel (c), as we only detect a shift of 8 eV in the energy separation between the triplet and the singlet levels at low temperature with respect to room temperature, and thus we do not

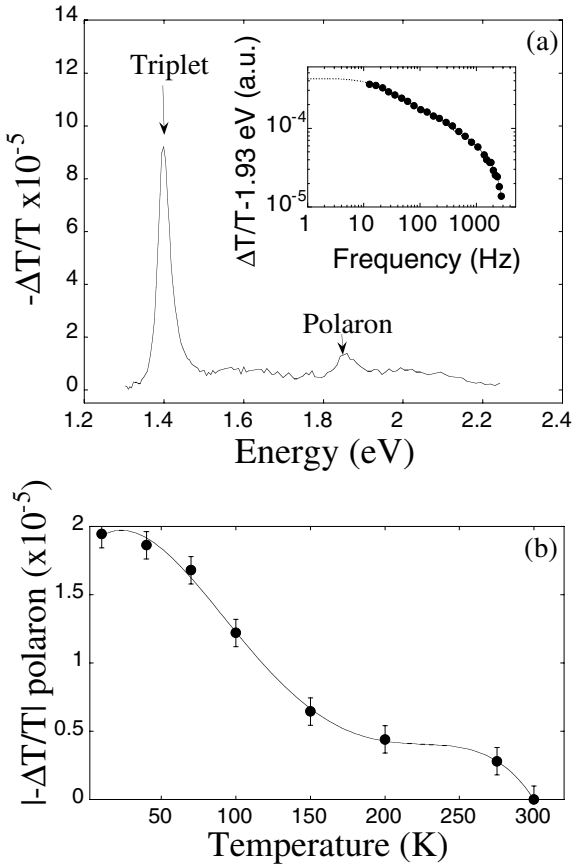

Figure 5. (a) The 77 K PA spectrum of a film containing β-phase chains. The inset shows the dependence of the polaron PA signal at 1.93 eV on the excitation modulation frequency. (b) The temperature dependence of the polaron PA signal at 1.93 eV. The solid curve is shown as a guide to the eye.

anticipate significant changes in the intersystem crossing rate. Moreover, were intersystem crossing a thermally activated process, it would become less important at low temperature rather than more important. We also note that earlier PA studies demonstrated that the triplet population at 70 K is some 8 times larger in as-SC glassy films than in films containing β-phase chains [23]. Thus, were channel (d) to be a dominant quenching mechanism, we would expect the PLQY of the as-SC film to be significantly lower than that of the β-phase film. As this is not observed, the only remaining possibility is that channel (e) (quenching by polarons) is the dominant additional non-radiative channel that becomes activated in low-temperature β-phase-containing PFO films.

To further investigate the importance of polaron quenching and its temperature dependence, we performed PA measurements on PFO films prepared with each of the four morphologies. These films were 5 ± 0.5 μm thick and were prepared by drop-casting rather than spin-coating. Figure 5(a) shows the 77 K PA spectrum measured for the β-phase-containing PFO film. The PA spectrum is characterized by two peaks, positioned at 1.93 and 1.43 eV. On the basis of previous work [23], we assign the transitions at 1.43 and at 1.93 eV to excited state absorption of triplet excitons and polarons respectively. We are able

to observe the triplet–triplet transition in our PA measurements on all four PFO morphologies (data not shown here). However, we only observe the polaron transition in films containing β-phase chains. It thus appears that the quasi-cw polaron population in β-phase-containing films is significantly higher than for any of the other film morphologies, and we propose that the β-phase chains stabilize polarons by acting as low-energy trapping sites. The polaron absorption does not appear in measurements on the other morphologies, presumably because the mobility of the polarons is much higher (due to the absence of traps), and this facilitates rapid polaron–polaron recombination. We note in this respect that polaron absorption has been previously observed in ultrafast pump–probe studies of as-SC PFO films. The polarons were found to have fast recombination dynamics, with a polaron lifetime of $\approx$80 ps [29]. This short lifetime is consistent with our observations.

Figure 5(b) plots the temperature dependence of the modulus of the in-phase and out-of-phase PA components ($|-\Delta T/T|$) at 1.93 eV for the β-phase-containing film. It can be seen that the polaron population increases monotonically as the temperature is decreased. It is instructive to calculate the polaron density on the β-phase chains from the PA measurement: we estimate the polaron population (n) from the change in transmission ($-\Delta T/T$) at 1.93 eV using

$$\frac{-\Delta T}{T} = nd\sigma \tag{2}$$

where d is the film thickness and σ the cross section for polaron absorption. Theoretical calculations have shown that the optical cross section for singlet excitons is comparable to that for polarons and low-lying triplets [30]. Given that the peak absorption coefficient for an as-SC film of PFO is $\alpha = 2.2 \times 10^5$ cm^{-1}, we can estimate the singlet ground state cross section using

$$\sigma = \frac{\alpha}{N} \tag{3}$$

where N is the number density of ground states. If we assume that each monomeric segment has an associated ground state, we can calculate N using

$$N = \frac{\rho}{m_w} N_A \tag{4}$$

where ρ is the film density, m_w is the molecular weight of the monomer, N_A is Avogadro's number. For PFO, $m_w = 388$ and $\rho = 1$ g cm^{-3}; we calculate $\sigma = 1.4 \times 10^{-16}$ cm^2. A value for the polaron absorption cross section in an MEH-PPV derivative has recently been measured as 7.5×10^{-17} cm^2 [31]. This is within a factor of two of our estimate for PFO. The thickness d in equation (2) has to be regarded as the thickness of the film region where the absorption takes place. Therefore it depends on the penetration depth of the laser and it may not coincide with the effective thickness of the sample. The extinction coefficient at 354 nm is approximately half of that calculated for the absorption maximum. This gives a penetration depth for the pump laser as about 100 nm. Taking into account exciton migration (a few tens of nanometres), we can estimate that all the absorption is taking place within half a micron of the surface, i.e. approximately one tenth of the total film thickness. In the deeper region of the film the pump laser intensity will be lower than 1% of the total, and therefore the absorption processes in this region can be neglected. Substituting our estimate for the cross section in equation (2), and using a PFO thickness of 5×10^{-5} cm for the drop-cast film that we have studied, gives a polaron density of 3.1×10^{15} cm^{-3} at 10 K.

This value however certainly underestimates the actual polaron population: it has been shown that the decay lifetime of polarons in β-phase-containing PFO films has two components: a fast component having a lifetime of 300 μs, and a slow component with a lifetime of 7 ms [32].

Our PA measurements were performed at a chopping frequency of 300 Hz ($\tau_{chop} = 3.3$ ms), and thus the lock-in technique used here is not sensitive to the polaron population having the long decay lifetime. The inset to figure 5(a) shows a previous measurement [32] of the in-phase $|-\Delta T/T|$ signal as a function of chopping frequency ω. The frequency dependence for $\Delta T/T$ assuming a monomolecular recombination process is given by

$$\left|\frac{\Delta T}{T}(\omega)\right| \propto \left[\frac{1}{1+(\omega\tau)^2} - \mathrm{i}\frac{\omega\tau}{1+(\omega\tau)^2}\right] G(\nu)\sigma\tau d \tag{5}$$

where τ is the lifetime of the species detected, $G(\nu)$ is the polaron generation rate at the pump energy, d is the film thickness, and σ is the polaron absorption cross section. The first term in equation (5) is the frequency dependence of the in-phase signal used to fit the data in the inset to figure 5(a). A reasonable fit is obtained assuming the polaron population decays with two characteristic lifetimes of 7 and 0.4 ms. We can thus extrapolate the steady-state $\Delta T/T(\omega\tau \ll 1)$, and we calculate that our measurement of the polaron population made at 300 Hz underestimates the actual polaron population by a factor of 3.6. We also assume that the polaron population that we detect is all located on β-phase chains since we do not detect any appreciable polaron population in quasi-cw PA measurements on as-drop-cast films. Noting that only 13% of the PFO chains adopt a β-phase conformation, we assume that the local density of polarons on β-phase chains is $\approx$7.7 times larger than is indicated by the bulk PA measurement. Combining these factors, we estimate that at 70 K, the polaron population on the β-phase chains is $\approx 8.6 \times 10^{16}$ cm^{-3}.

To interpret the significance of this measurement, we note the result of List *et al* [33], that for the related polymer Me-LPPP, a polaron population of 10^{17} cm^{-3} will quench the singlet excitons at a rate (k_{pol}) equal to the radiative rate of the singlets (k_{rad}), i.e. $k_{pol} = k_{rad}$. We can estimate the polaron quenching rate in β-phase PFO films at low temperature using our quantum efficiency measurements. The PLQY at temperature T is given by

$$\Phi^T = \frac{k_{rad}}{k_{rad} + k_{nr}^T + k_{pol}^T} \tag{6}$$

where k_{nr} is the quenching rate due to other non-radiative channels, and the superscript indicates temperature. We first assume that quenching by polarons is only important at low temperature. We are confident that this assumption is valid, since our PA measurements do not detect any polaron absorption at room temperature within the sensitivity of our experimental set-up (see figure 5(b)). Thus the only polaron quenching term that is not equal to zero is $k_{pol}^{\beta\ 10\ \mathrm{K}}$, where the additional superscript, β, denotes the morphology of the PFO film. We also make the common assumption that the radiative rates at room temperature and at low temperature are identical [33]. It is trivial to show that for the as-SC film

$$\frac{k_{nr}^{SC\,298\,\mathrm{K}}}{k_{nr}^{SC\,10\,\mathrm{K}}} = \frac{\left[\frac{1}{\Phi^{SC\,10\,\mathrm{K}}} - 1\right]}{\left[\frac{1}{\Phi^{SC\,298\,\mathrm{K}}} - 1\right]} = 4.0. \tag{7}$$

Thus as anticipated from the PLQY measurements, the non-radiative channels in the as-SC PFO film decrease as the temperature is lowered due to hindered exciton migration to non-radiative quenching sites. Whether the same model can be applied to excitons in a β-phase-containing film is not clear. To a first approximation, we assume that the excitons created on the polymer chains in the glassy matrix surrounding the β-phase chains transfer to them much more rapidly than they explore the rest of the matrix and find a non-radiative defect. This scenario is supported by the steady-state PL spectra (see above) that show almost complete exciton transfer to the lower-energy-gap β-phase chains, even if the film contains only a 1 or 2% fraction of these chains. Once an exciton has transferred to a β-phase chain, it is effectively localized, and thus any changes in the non-radiative rates that occur for the matrix

chains due to thermally assisted exciton migration to defect sites are no longer especially significant. Our model might at first seem to neglect changes that could occur in the non-radiative rates associated with defect states on β-phase chains. However, the presence of a defect on a β-phase chain would have the effect of increasing the HOMO–LUMO gap of that chain segment and effectively rendering it no longer an effective exciton trap. Indeed, the emissive β-phase chains must by definition be defect free. We can thus write $k_{nr}^{\beta\,\mathrm{RT}} \approx k_{nr}^{\beta\,10\,\mathrm{K}}$, which implies

$$\frac{k_{pol}^{\beta\,10\,\mathrm{K}}}{k_{rad}} = \frac{1}{\Phi^{\beta\,10\,\mathrm{K}}} - \frac{1}{\Phi^{\beta\,298\,\mathrm{K}}} \approx 0.5. \tag{8}$$

We thus estimate that a polaron population of 5×10^{16} cm^3 is sufficient to cause the 20% drop that we observe in the PLQY of the β-phase PFO film as the temperature is reduced from room temperature to 10 K. It can be seen that this is in very reasonable agreement with our estimation of the polaron population at 10 K in the β-phase (8.6×10^{16} cm^{-3}) that we determine from PA measurements.

We therefore propose the following picture for PLQY quenching in the β-phase-containing samples at low temperature: the β-phase chains are uniformly dispersed in a glassy matrix of polymer chains with shorter conjugation lengths. Excitons photoexcited on the glassy matrix polymer can transfer via thermally assisted migration and via Förster transfer to β-phase chains, from whence they decay radiatively [25, 26]. This transfer process is almost complete *even* at low temperature, since dipole–dipole coupling is temperature independent. When an exciton transfers onto a β-phase chain it has excess energy and can dissociate via a charge-transfer process to form a polaron pair. At room temperature, polarons can easily escape from the β-phase chains back to the surrounding matrix, where they can combine with polarons of the opposite charge to reform an exciton. At low temperatures however, polarons become localized on the β-phase chains as the rate of backscattering to the matrix is reduced. The spatial coincidence between the stabilized polarons and relaxed excitons on the β-phase chains results in a significant quenching of fluorescence and thus a reduction in the PLQY. Because of the long polaron lifetime, which is estimated to be 7 ms at 77 K for as-SC PFO films [32], one polaron is able to quench many excitons before it recombines with a polaron of the opposite charge.

In conclusion, we have studied the influence of morphology on the temperature-dependent PLQY of PFO. Films with four different morphologies, namely 'as-SC glass', 'quenched nematic glass', 'crystalline', and 'vapour-treated SC glass containing a fraction of 2_1 helix conformation (β-phase) chains'. We find significant differences in PLQY between these morphologies of PFO and show that whilst in the first three cases, the PLQY increases as the temperature decreases, for the films containing β-phase chains, the PLQY decreases with decreasing temperature. The increase in PLQY in the crystalline, nematic glass, and as-SC films can be explained as a consequence of hindered exciton migration towards quenching sites at low temperature. The corresponding PLQY reduction for the films containing β-phase chains is attributed to the annihilation of singlet excitons by polarons that become trapped on these highly conjugated polymer segments.

Acknowledgments

DGL and MA thank the UK Engineering and Physical Sciences Research Council (EPSRC) for the provision of, respectively, an *Advanced Research Fellowship* and a PhD studentship. MA also thanks the Sardinian Regional Government of Italy for a bursary award. The authors thank Mark Bernius of the Dow Chemical Company (USA) for providing the PFO polymer

used in this work, the UK EPSRC for support via research grant GR/M21201 and Emil List for very fruitful discussions.

References

[1] Burroughes J H, Bradley D D C, Brown A R, Marks R N, Mackay K, Friend R H, Burn P L and Holmes A B 1990 *Nature* **347** 539–41
[2] See http://www.CDTLtd.co.uk, http://www.kodak.com, http://www.components.philips.com for latest results
[3] Fukuda Y, Watanabe T, Wakimoto T, Miyaguchi S and Tsuchida M 2000 *Synth. Met.* **111–2** 1–6
[4] Ho P K H, Kim J S, Burroughes J H, Becker H, Li S F Y, Brown T M, Cacialli F and Friend R H 2000 *Nature* **404** 481–4
[5] Cao Y, Yu G, Parker I D and Heeger A J 2000 *J. Appl. Phys.* **88** 3618–23
[6] Yu W L, Cao Y, Pei J A, Huang W and Heeger A J 1999 *Appl. Phys. Lett.* **75** 3270–2
[7] Grice A W, Bradley D D C, Bernius M T, Inbasekaran M, Wu W W and Woo E P 1999 *Appl. Phys. Lett.* **73** 629–31
[8] Fletcher R B, Lidzey D G, Bradley D D C, Walker S, Inbasekaran M and Woo E P 2000 *Synth. Met.* **111–2** 151–3
[9] Jiang X Z, Liu Y Q, Song X Q and Zhu D B 1997 *Synth. Met.* **91** 311–13
[10] Lidzey D G, Alvarado S F, Seidler P F, Bleyer A and Bradley D D C 1997 *Appl. Phys. Lett.* **71** 2008–10
[11] Horowitz G and Hajlaoui M E 2000 *Synth. Met.* **122** 185–9
[12] Hutten P F and Hadziioannou G 1999 *Semiconducting Polymers* (Weinheim: Wiley–VCH) pp 602–4
[13] Campbell I H and Ferraris J P 1996 *J. Appl. Phys.* **80** 2883–90
[14] Grell M, Bradley D D C, Ungar G, Hill J and Whitehead K S 1999 *Macromolecules* **32** 5810–17
[15] Ariu M, Lidzey D G and Bradley D D C 2001 *Synth. Met.* **116** 217–21
[16] Ariu M, Lidzey D G and Bradley D D C 2000 *Synth. Met.* **111–2** 607–10
[17] Lieser G, Oda M, Miteva T, Meisel A, Nothofer H, Scherf U and Neher D 2000 *Macromolecules* **33** 4490–5
[18] Greenham N C, Samuel I D W, Hayes G R, Phillips R T, Kessener Y A R R, Moratti S C, Holmes A B and Friend R H 1995 *Chem. Phys. Lett.* **241** 89–96
[19] Mei P, Murgia M, Taliani C, Lunedei E and Muccini M 2000 *J. Appl. Phys.* **88** 5158–65
[20] Marks R N, Michel R H, Gebauer W, Zamboni R, Taliani C, Mahrt R F and Hopmeier M 1998 *J. Phys. Chem.* B **102** 7563–7
[21] Muccini M, Murgia M, Taliani C, degli Esposi A and Zamboni R 2000 *J. Opt. A: Pure Appl. Opt.* **2** 577–83
[22] Wan V 2001 *PhD Thesis* Cavendish Laboratory, University of Cambridge
[23] Cadby A J, Lane P A, Mellor H, Martin S J, Grell M, Giebeler C, Bradley D D C, Wohlgenannt M, An C and Vardeny Z V 2000 *Phys. Rev.* B **62** 15 604–9
[24] Virgili T, Lidzey D G and Bradley D D C 2000 *Adv. Mater.* **12** 58–62
[25] Buckley A R, Rahn M D, Hill J, Cabanillas-Gonzalez J, Fox A M and Bradley D D C 2001 *Chem. Phys. Lett.* **339** 331–6
[26] List E J W, Creely C, Leising G, Schulte N, Schlüter A D, Scherf U, Müllen K and Graupner W 2000 *Chem. Phys. Lett.* **325** 132–8
[27] List E J W, Partee J, Shinar J, Scherf U, Müllen K, Zojer E, Petritsch K, Leising G and Graupner W 2000 *Phys. Rev.* B **61** 10807–14
[28] Shinar J 1996 *Synth. Met.* **78** 277–84
[29] Stevens M, Silva C, Russell D M and Friend R H 2001 *Phys. Rev.* B **63** 165213/1–18
[30] Zojer E, Cornil J, Leising G and Brèdas J L 1999 *Phys. Rev.* B **59** 7957–68
[31] Dhoot A S 2001 *PhD Thesis* Darwin College, University of Cambridge
[32] Cadby A J 2001 *PhD Thesis* University of Sheffield
[33] List E J W, Kin C H, Naik A K, Scherf U, Leising G, Graupner W and Shinar J 2001 *Phys. Rev.* B **64** 155204/1–11